Out-of-Plane $(e, 2e)$ Experiments on Helium $L = 0, 1, 2$ Autoionizing Levels

B. A. deHarak,[1] K. Bartschat,[2] and N. L. S. Martin[1]

[1]*Department of Physics and Astronomy, University of Kentucky, Lexington, Kentucky 40506-0055, USA*
[2]*Department of Physics and Astronomy, Drake University, Des Moines, Iowa 50311, USA*

(Received 11 September 2007; published 11 February 2008)

Out-of-plane $(e, 2e)$ measurements are reported for the helium autoionizing levels $(2s^2)^1S$, $(2p^2)^1D$, $(2s2p)^1P$, and for direct ionization. While the recoil peak almost vanishes in the angular distribution for direct ionization, it remains significant for the autoionizing levels and exhibits a characteristic shape for each orbital angular momentum $L = 0, 1, 2$. A second-order model in the projectile-target interaction correctly reproduces the observed magnitudes of the recoil peaks, but is a factor of 2 too large in the central out-of-plane region.

DOI: 10.1103/PhysRevLett.100.063201 PACS numbers: 34.80.Dp

There has been much recent interest in two types of experiments on atomic ionization by charged-particle impact. This interest is fueled by the fact that sophisticated theories failed to reproduce the experimental results of out-of-plane experiments on He direct ionization at high incident projectile energies (where even first-order theories were expected to be adequate) [1,2], and coplanar experiments on He ionization-excitation [3–5]. In an out-of-plane experiment, the (slow) electron ejected with momentum $\vec{k}_{\rm ej}$ is observed in directions that do not lie in the scattering plane formed by the incident and (fast) scattered projectile momenta, $\vec{k}_0$ (energy E_0) and $\vec{k}_{\rm sc}$, respectively. In the more traditional coplanar experiments, all three momenta lie in the same plane. The experiments of interest here measure the triply differential cross section (TDCS) $d^3\sigma/d\hat{k}_{\rm ej}d\hat{k}_{\rm sc}dE_0$ (either absolute or relative) for fixed $\vec{k}_0$ and $\vec{k}_{\rm sc}$, i.e., the angular distribution of ejected electrons in coincidence with the scattered projectile. If the latter is an electron, the experiments are of the $(e, 2e)$ type. Over the past 30 years, computational techniques have improved to the extent that there is now good agreement between theoretical predictions and coplanar data for simple target systems such as H and He. A discussion of the current state of theoretical calculations for these processes can be found, for example, in [6]. As stated above, some recent out-of-plane experiments, however, have been poorly described by theory. Of particular interest here are those experiments with high incident energies. For these the plane-wave Born approximation (PWBA) may be used to illustrate the expected *qualitative* features of the TDCS.

Figure 1 shows a 3D cartoon of a representative PWBA calculation for direct ionization. The ejected electron intensity in a particular direction is proportional to the position vector to the surface in that direction. In the PWBA the angular distribution of the ejected electrons is rotationally symmetric around the momentum transfer $\vec{K} \equiv \vec{k}_0 - \vec{k}_{\rm sc}$, with a large lobe (the *binary peak*) in the $+\hat{K}$ direction, and a much smaller lobe (the *recoil peak*) in the $-\hat{K}$ direction (typically for $K \gtrsim 0.7$ a.u.). In the figure, plane I corresponds to a coplanar experiment, and plane II is perpendicular to $\vec{K}$ and the scattering plane. In a recent experiment on He ionization by fast C^{6+} ions [1], the angular distribution of electrons ejected into plane I agreed well with theory, but the experimental results in plane II disagreed with expectations by a factor of between 3 and 5; no calculations to date have been able to satisfactorily reproduce these data. Somewhat smaller discrepancies were found in an $(e, 2e)$ experiment carried out with equivalent kinematics [2]. Out-of-plane experiments on Mg [7,8] found dramatic deviations from the rotational symmetry about $\vec{K}$.

These experiments on He direct ionization are examples of three-body dynamics because the $1s$ electron common to the initial state and the residual ion is essentially a spectator [5]. Helium ionization-excitation on the other hand, where the ion is left in an excited state, is a four-

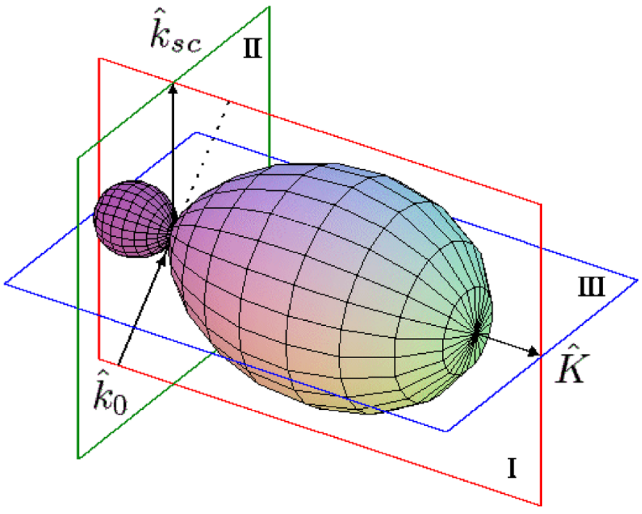

FIG. 1 (color online). Representative PWBA calculation of an ejected electron angular distribution for direct ionization. See text for details.

body process and hence presents a much greater challenge to theory; coplanar experiments have recently investigated this process [3–5]. It was found that second-order models in the projectile-target interaction were essential to get good agreement when the two outgoing electrons had different energies. However, even these theories did not do so well for the case of symmetric energy sharing [9]. In fact, even the calculation of the total He ionization-excitation cross section remains a significant problem [10].

Here we present the first out-of-plane experiments on autoionizing levels, namely, the three singlet He levels $(2s^2)^1S$, $(2p^2)^1D$, and $(2s2p)^1P$. This process may be written as

$$\begin{array}{ccc} \mathrm{He}(1s^2) + e_0 & \longrightarrow & \mathrm{He}^+(1s) + e_{sc} + e_{ej}, \\ & \searrow\ \mathrm{He}\ (2\ell 2\ell')\ \nearrow & \end{array} \tag{1}$$

where there is interference between the amplitudes for direct ionization (upper path) and autoionization via an intermediate resonance (lower path) [11]. Since He autoionization by electron impact involves both direct ionization and the excitation of doubly excited resonances, it is an example of mixed three-body and four-body processes. Our experiments therefore test how well theory can describe three-body *and* four-body dynamics for out-of-plane kinematics. Table I lists the properties of the three singlet He $2\ell 2\ell'$ autoionizing levels with orbital angular momentum $L = 0, 1, 2$ [12–14]. These have been extensively studied in coplanar geometry using the $(e, 2e)$ technique [15–18]. The experiments were analyzed by fitting them to the TDCS to yield the angular dependence of three parameters that describe the line profile of each resonance. The out-of-plane experiments reported in this Letter are somewhat simpler: we examine the gross effects of autoionization on the ejected electron angular distribution after summing the data across a resonance.

We carried out $(e, 2e)$ out-of-plane experiments for the special kinematical case where the momentum transfer vector is perpendicular to the scattered electron direction. The condition for this is $\theta_{sc} = \arcsin(\sqrt{\Delta E/E_0})$, where ΔE is the energy lost by the incident electron; for an autoionizing level $\Delta E = E_L$. The corresponding momentum transfer is $K = \sqrt{2\Delta E}$, independent of the initial energy.

TABLE I. Helium autoionizing levels and relevant parameters obtained from the literature [12–14]. The energy above the ground state is E_L, where L is the orbital angular momentum of the level, E_{ej} is the corresponding ejected electron energy, and Γ_L is the level width.

	E_L (eV)	E_{ej} (eV)	Γ_L (meV)
$2s^2\,{}^1S_0$	57.84	33.25	120
$2p^2\,{}^1D_2$	59.91	35.32	57
$2s2p\,{}^1P_1$	60.15	35.56	38

With these kinematics we measured the $(e, 2e)$ out-of-plane angular distribution of ejected electrons corresponding to plane III of Fig. 1. This plane contains the momentum transfer vector $\vec{K}$; it is perpendicular to $\vec{k}_{sc}$ and hence also to the scattering plane. (Note that all ejected electron directions $\hat{k}_{ej}$ in plane III are perpendicular to $\hat{k}_{sc}$.) Our experiments were carried out with an incident electron energy $E_0 = 488$ eV and a corresponding scattering angle $\theta_{sc} = 20.5°$ for an energy loss of ≈ 60 eV and a momentum transfer $K = 2.1$ in the autoionizing region.

We performed three types of calculations for comparison with the experimental data: a simple PWBA calculation and sophisticated first-order and second-order hybrid distorted-wave + convergent R-matrix with pseudostates (close-coupling) calculations (DWB1-RMPS and DWB2-RMPS, respectively). Details of the latter methods are given elsewhere [19–22]. The essential point is that the (fast) projectile-target interaction is treated perturbatively to first (DWB1) or second (DWB2) order, while the initial bound state and the e-He^+ half-collision of a slow ejected electron and the residual ion are treated via a convergent close-coupling expansion. While the PWBA model is not expected to be quantitatively correct, it is useful in that the formalism developed by Balashov *et al.* [23] makes definite qualitative predictions about the effect of autoionization on the $(e, 2e)$ ejected electron angular distributions. Specifically, the TDCS in the neighborhood of an isolated autoionizing resonance of angular momentum L is given (in atomic units) by

$$\frac{d^3\sigma}{d\hat{k}_{ej}\,d\hat{k}_{sc}\,dE_0} = \frac{4}{K^4}\frac{k_{sc}}{k_0}|T(\vec{k}_{ej}, \vec{K})|^2, \tag{2}$$

where the amplitude is

$$T(\vec{k}_{ej}, \vec{K}) = t(\vec{k}_{ej}, \vec{K}) + t^{(L)}(\vec{k}_{ej}, \vec{K})\frac{q_L - i}{\varepsilon_L + i}. \tag{3}$$

Here q_L is the Fano resonance profile index [11] and ε_L is the energy away from the resonance position in units of the resonance half-width $\Gamma_L/2$. The direct ionization amplitude is $t(\vec{k}_{ej}, \vec{K})$, while $t^{(L)}(\vec{k}_{ej}, \vec{K})$ is the part of the direct ionization amplitude associated with the resonance. The latter is given by

$$t^{(L)}(\vec{k}_{ej}, \vec{K}) = c_L P_L(\cos\theta_0), \tag{4}$$

with

$$c_L = \frac{\int t(\vec{k}_{ej}, \vec{K}) P_L(\cos\theta_0)\, d\hat{k}_{ej}}{\int P_L(\cos\theta_0)^2\, d\hat{k}_{ej}}, \tag{5}$$

where P_L is a Legendre polynomial and θ_0 is the angle between the ejected electron direction and the momentum transfer vector: $\cos\theta_0 = \hat{k}_{ej} \cdot \hat{K}$. Details of our method for calculating $t(\vec{k}_{ej}, \vec{K})$, when plane waves are used to describe the incident, scattered, and ejected electrons, are given in

[24]. In our model, q_L was left as an adjustable parameter to be fitted to the experimental data. For direct ionization, the PWBA and all other theories predict that as K increases the intensity of the recoil peak decreases relative to that of the binary peak, and for the kinematics of the present experiment ($K \approx 2$) it essentially vanishes. However, when autoionization is present the second term in Eq. (3) does not vanish. The recoil peak, therefore, remains significant and exhibits a specific shape determined by the angular momentum L of the autoionizing state via the P_L dependency of $t^{(L)}(\vec{k}_{\rm ej}, \vec{K})$. Thus each of the three He autoionizing levels ($L = 0, 1, 2$) is expected to leave a characteristic signature in the shape of a recoil peak with behavior given by $(P_L)^2$.

The experimental apparatus is described in detail elsewhere [18,25]; its geometry is shown in Fig. 2. Two ejected electron detectors are positioned at $\pm 90°$ with respect to the scattered electron detector; all three lie in the same plane. The gun moves on the surface of a cone, with axis $\hat{k}_{\rm sc}$, of half-angle equal to the scattering angle $\theta_{\rm sc}$. This is equivalent to rotating the ejected electron detectors around $\hat{k}_{\rm sc}$ (in plane III of Fig. 1) while keeping the gun and scattered electron detector fixed. For the present experiments the apparatus was tuned to accept electrons in a uniform energy window of 0.4 eV [18]; the theoretical calculations were energy integrated over the same window. Figure 3 exhibits our experimental results and theoretical predictions; $\theta_0 = 0$ is the binary peak position (i.e., momentum transfer direction) and $\theta_0 = 180°$ is the recoil peak position—all other angles lie outside the scattering plane (see plane III of Fig. 1). All experimental data and calculations were normalized to unity at the binary peak. Figure 3(a) is the angular distribution for direct ionization. The PWBA underestimates the width of the binary peak, whereas both the DWB1-RMPS and DWB2-RMPS calculations are in good agreement with experiment over the entire angular range, within the statistics of the present experiment. The data show conclusively that the recoil peak is extremely small, and we therefore expect autoionization to have a profound effect on this part of the angular distribution. That this is indeed the case is seen in Figs. 3(b)–3(d), which show the angular distributions of the ^1S, ^1D, and ^1P autoionizing levels. For the PWBA calculations, values of q_L were chosen to give the correct recoil peak intensities. The resultant curves agree quite well with the experimental data, with fitted values

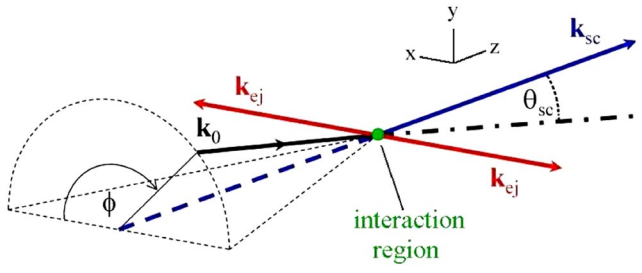

FIG. 2 (color online). Geometry of the apparatus. The incident ($\mathbf{k}_0$) and detected ejected ($\mathbf{k}_{\rm ej}$) and scattered ($\mathbf{k}_{\rm sc}$) electron directions are indicated.

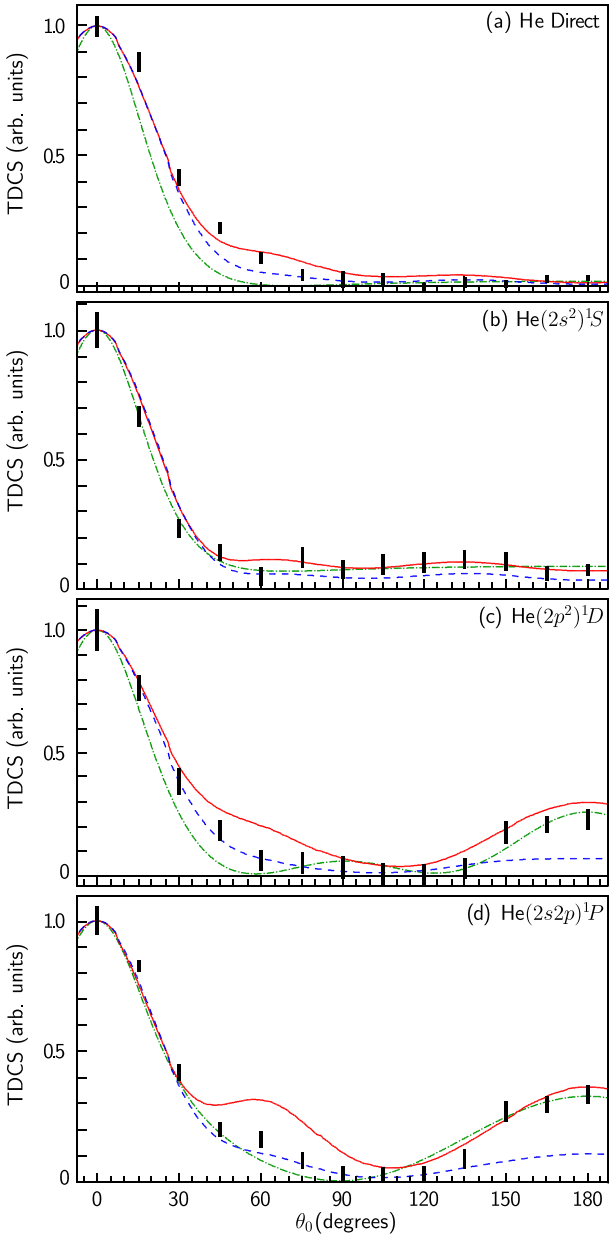

FIG. 3 (color online). Helium out-of-plane (e, $2e$) ejected electron angular distributions for 488 eV electrons scattered through 20.5°. The vertical bars represent the experimental results and include both statistical and systematic errors. (a) Direct ionization with 34.1 eV ejected electrons. (b)–(d) Direct ionization plus autoionization via $(2s^2)^1S$, $(2p^2)^1D$, $(2s2p)^1P$. The solid (red) and dashed (blue) lines are DWB2-RMPS and DWB1-RMPS calculations, respectively, while the chained (green) lines are fitted PWBA calculations described in the text. Theory and experiment are normalized to unity at $\theta_0 = 0$.

$q_0 = -15$, $q_1 = -6.3$, and $q_2 = -4.8$. These are larger by factors of between three and eight than first-order calculated values found in the literature [26]—this possibly indicates the need for a second-order calculation of q_L which treats the four-body projectile-target interaction more completely. As predicted, a comparison of the PWBA calculations with the data shows that each autoionizing level has a signature determined by the behavior of the appropriate $(P_L)^2$. In Fig. 3(b) the data for ^1S are clearly nonzero over the entire angular range, as expected from $(P_0)^2 =$ constant. Both the ^1D and ^1P angular distributions in Figs. 3(c) and 3(d) show pronounced recoil peaks and minima close to 90°, and the data in the range $\theta_0 = 60° \rightarrow 135°$ are consistent with the behavior of $(P_2)^2$ and $(P_1)^2$, respectively. The first-order DWB1-RMPS model does a good job for $\theta_0 = 45° \rightarrow 135°$, but it severely underestimates the magnitudes of the recoil peaks. On the other hand, the second-order DWB2-RMPS calculations are in excellent agreement with the data in the recoil peak for all three autoionizing levels, but are about a factor of 2 too large in the out-of-plane region $\theta_0 = 45° \rightarrow 90°$ for the ^1D and ^1P levels. Note that when autoionization is *absent* these two theories also disagree by a factor of 2 in this region [see Fig. 3(a)]. This may be responsible, via the interference term, for the similar disagreement in Figs. 3(c) and 3(d).

In summary, we have measured out-of-plane angular distributions for He direct ionization and $L = 0, 1, 2$ autoionizing levels. For direct ionization, a three-body process, both first-order and second-order distorted-wave calculations give an adequate description, as was true for out-of-plane experiments on Mg [7,8]. We find that the presence of autoionization has a dramatic effect on the angular distribution, as predicted by Balashov *et al.* [23], with each autoionizing resonance presenting its own, L-dependent, "signature." In a comparison of experiment and theory two regions are of particular interest: a central, fully out-of-plane, region $\theta_0 = 45° \rightarrow 135°$, and the recoil peak, $\theta_0 = 135° \rightarrow 180°$, which intersects the coplanar region along $-\hat{K}$. For an incident energy of 488 eV and a momentum transfer of 2.1 a.u., we find that a second-order model in the projectile-target interaction is necessary to correctly reproduce the magnitude of the recoil peak when autoionization is present; the corresponding first-order model underestimates the magnitude by a factor of 3. This need for a higher-order description is consistent with the findings of the excitation-ionization experiments (i.e., four-body processes) mentioned above [3–5]. However, neither the DWB2-RMPS nor the DWB1-RMPS model is able to reproduce the data over the full $0 \rightarrow 180°$ out-of-plane range; DWB2-RMPS is good in the recoil peak but not satisfactory in the central region while the opposite is true for DWB1-RMPS. For our kinematics, therefore, we conclude that current sophisticated theories are still not entirely adequate for out-of-plane experiments on He autoionization.

This work was supported by the United States National Science Foundation under Grants No. PHY-0555541 (N. L. S. M.) and No. PHY-0244470 (K. B.).

[1] M. Schulz, R. Moshammer, D. Fischer, H. Kollmus, D. H. Madison, S. Jones, and J. Ullrich, Nature (London) **422**, 48 (2003).
[2] M. Dürr, C. Dimopoulou, B. Najjari, A. Dorn, and J. Ullrich, Phys. Rev. Lett. **96**, 243202 (2006).
[3] G. Sakhelashvili, A. Dorn, C. Höhr, J. Ullrich, A. S. Kheifets, J. Lower, and K. Bartschat, Phys. Rev. Lett. **95**, 033201 (2005).
[4] S. Bellm, J. Lower, and K. Bartschat, Phys. Rev. Lett. **96**, 223201 (2006).
[5] S. Bellm, J. Lower, K. Bartschat, X. Guan, D. Weflen, M. Foster, A. L. Harris, and D. H. Madison, Phys. Rev. A **75**, 042704 (2007).
[6] M. Dürr, C. Dimopoulou, A. Dorn, B. Najjari, I. Bray, D. V. Fursa, Z. Chen, D. H. Madison, K. Bartschat, and J. Ullrich, J. Phys. B **39**, 4097 (2006).
[7] R. W. van Boeyen, N. Watanabe, J. W. Cooper, J. P. Doering, J. H. Moore, and M. A. Coplan, Phys. Rev. A **73**, 032703 (2006).
[8] M. Foster, J. L. Peacher, M. Schulz, D. H. Madison, Z. Chen, and H. R. J. Walters, Phys. Rev. Lett. **97**, 093202 (2006).
[9] K. Bartschat, I. Bray, D. V. Fursa, and A. T. Stelbovics, Phys. Rev. A **76**, 024703 (2007).
[10] O. K. Vorov and K. Bartschat, J. Phys. B **38**, 1189 (2005).
[11] U. Fano, Phys. Rev. **124**, 1866 (1961).
[12] K. Schulz, G. Kaindl, M. Domke, J. D. Bozek, P. A. Heimann, A. S. Schlachter, and J. M. Rost, Phys. Rev. Lett. **77**, 3086 (1996).
[13] J. P. van den Brink, G. Nienhuis, J. van Eck, and H. G. M. Heideman, J. Phys. B **22**, 3501 (1989).
[14] B. A. deHarak, J. G. Childers, and N. L. S. Martin, Phys. Rev. A **74**, 032714 (2006).
[15] A. Crowe, D. G. McDonald, S. E. Martin, and V. V. Balashov, Can. J. Phys. **74**, 736 (1996).
[16] M. J. Brunger, O. Samardzic, A. S. Kheifets, and E. Weigold, J. Phys. B **30**, 3267 (1997).
[17] O. Samardzic, L. Campbell, M. J. Brunger, A. S. Kheifets, and E. Weigold, J. Phys. B **30**, 4383 (1997).
[18] B. A. deHarak, J. G. Childers, and N. L. S. Martin, J. Electron Spectrosc. Relat. Phenom. **141**, 75 (2004).
[19] K. Bartschat and P. G. Burke, J. Phys. B **20**, 3191 (1987).
[20] R. H. G. Reid, K. Bartschat, and A. Raeker, J. Phys. B **31**, 563 (1998); J. Phys. B **33**, 5261(E) (2000).
[21] Y. Fang and K. Bartschat, J. Phys. B **34**, L19 (2001).
[22] K. Bartschat and A. N. Grum-Grzhimailo, J. Phys. B **35**, 5035 (2002).
[23] V. V. Balashov, S. S. Lipovetskiĭ, and V. S. Senashenko, Sov. Phys. JETP **36**, 858 (1973).
[24] B. A. deHarak, Z. Chen, D. H. Madison, and N. L. S. Martin, J. Phys. B **38**, L145 (2005).
[25] B. A. deHarak and N. L. S. Martin, Meas. Sci. Technol. **19**, 015604 (2008).
[26] A. S. Kheifets, J. Phys. B **26**, 2053 (1993).